MATTER: International Journal of Science and Technology
ISSN 2454-5880

Borisenok & Ünal, 2017

Volume 3 Issue 2, pp. 560-576

Date of Publication: 10th November 2017

DOI-https://dx.doi.org/10.20319/mijst.2017.32.560576

This paper can be cited as: Borisenok, S., & Ünal, Z. (2017). Tracking of Arbitrary Regimes for Spiking and Bursting in the Hodgkin-Huxley Neuron. MATTER: International Journal of Science and Technology, 3(2), 560-576.

TRACKING OF ARBITRARY REGIMES FOR SPIKING AND BURSTING IN THE HODGKIN-HUXLEY NEURON

Sergey Borisenok
Department of Electrical and Electronics Engineering, School of Engineering, Abdullah Gül University, Kocasinan - 38080 Kayseri, Turkey
sergey.borisenok@agu.edu.tr

Zeynep Ünal
Department of Electrical and Electronics Engineering, School of Engineering, Abdullah Gül University, Kocasinan - 38080 Kayseri, Turkey
zeynepsenel51@gmail.com

Abstract

We propose here efficient mathematical tracking control algorithms to design the spiking or bursting behavior in the four dimensional dynamical system modeling biological neurons represented by the Hodgkin-Huxley (HH) differential equations. The stimulating external electrical current serves as a control signal, while the membrane action potential is the target output. We use two alternative feedback algorithms, Fradkov's speed gradient and Kolesnikov's 'synergetic' target attractor control, to produce arbitrary spiking or bursting regimes in the model and to track the action potential of the system. Both algorithms demonstrate high efficiency and robustness for the controlled HH dynamics. For virtually any initial condition we are able to form a single spike at the chosen moment of time, the train with any number of spikes, the arbitrary-shaped burst, and also to switch between regular and chaotic regimes of bursting.

Two approaches developed here could be easily adopted for the networks of neural clusters and used effectively for the purposes of neuro-informatics and for modeling neural dysfunctions like epileptiform or other abnormal behavior in Hodgkin-Huxley neuron clusters. This work has been supported by the TÜBİTAK project 116F049 "Controlling Spiking and Bursting Dynamics in Hodgkin-Huxley Neurons".

Keywords

Hodgkin-Huxley Neuron, Neuron Spiking and Bursting, Feedback, Tracking Control, Speed Gradient, Target Attractor Feedback

1. Introduction

Biological neurons demonstrate variety of complex dynamical behavior that includes intermittency between resting and spiking at the different time scales (Rabinovich & Abarbanel, 1998; Purali, 2002; DiLorenzo & Victor, 2013). This intermittency causes their bursting properties, provides the communication among the cells and forms a basis for the information processing in biological networks.

The mechanisms of such irregular behavior are originated in the inner structure of neurons and in the architecture of their networks as well. In the bursting regime the neuron, stimulating by external electrical currents (signals) coming to its dendrites from the companion cells and by internal information treating processes in its own soma, produces in its axon an intensive spike train or several spikes or just one. Bursting is a quasi-periodical process, and usually it has a chaotic dynamical character (Strogatz, 1994; Cymbalyuka, et al., 2005).

Networks with spiking neurons play an important role in many applications of pattern recognition (Awadalla & Sadek, 2012) and computational algorithms (Bower, 2013; Brody & Hopfield, 2003). Neural populations demonstrate wide diapason of their flexible feedback for changes in the input stimuli. These adaptations help optimize the transmission of information about sensory inputs (Rasmussen, et al., 2017). Modeling of real systems demands computational neural network algorithms dealing with multi criteria decision making method (Lu, Tucciarone, et al., 2017; Saha, et al., 2017).In the frame of such algorithms the control of neuron spiking is a central subject of neuroscience (Moss & Gielen, 2001; Bandopadhayay & Stiles, 2017), particularly for learning processes (Bower, 2013; Qiao, et al., 2015).

Theoretical modelsproposed for spiking neuronscover virtually all areas of modern mathematics. Mostly they are formulated in the terms of multi-dimensional systems of ordinary differential equations.

In our paper we study feedback control algorithms applied to the most popular mathematical model of real neuron, the Hodgkin-Huxley dynamical system.

1.1. Review of Feedforward and Feedback Driven Control Methods for Neuron Dynamics

To drive the dynamical regime of the neuron, the electrical current *I* stimulating the membrane plays a role of an external control parameter. Usually this control current has been taken as a constant or a simple step-type function. Open-loop (feedforward) approachhas been used in (Fourcaud-Trocme, et al., 2003) for the linear response model with noisy input that combines fluctuations with a small harmonic component. The similar combination of feed forward designed pulses with the small noise applied to the Hodgkin-Huxley model was studied in (Danzl & Moehlis, 2008). A regular aperiodic high-frequency control signal was applied in (Qin et al., 2013). The set of open-loop control signals for the planar case has been reviewed in (Izhikevich, 2000); the corresponding detailed stability analysis one can find for a single neuron (Haddad, et al., 2014) and for dynamical networks of several neurons (Schultheiss, et al., 2011).

Majority of control feedforward algorithms applied to neuronal models are related to spike train design with the fixed shapes of the spikes, but with the variation over the inter-spike intervals and the number of pulses in the train. For instance, an optimal control scheme was performed in (Ahmadian, et al., 2011), where the control current *I*, consisted of the sequence of rectangular pulses, was limited in its amplitude. Alternative analysis (for a simplified 1-dimensional reduced model) was given in (Nabi & Moehlis, 2012). Adapted inverse control on spike train with delay was developed in (Li, et al., 2013). Also we should mention the Spike Response Model (Jolivet, et al., 2003) that predicts spikes in-vivo.

For multidimensional models, like HH, there are extra possibilities to manipulate with their nonlinear dynamics: the choice of an appropriate constant current *I* shifts an existing Hopf bifurcation or creates a new one (Ding & Hou, 2010).

Feedback (closed-loop) approachhas been used experimentally for stimulation of a particular regime of non-monotonic firing response (Lewis, et al., 2007).

For cellular systems the non-linear control algorithms have been recently developed in the form of Particle Swarm Optimization (Subashini, et al., 2017).

1.2. The Hodgkin-Huxley Model for Neuron Dynamics

One of the most popular ODE models for a single neuron has been derived phenomenologically in (Hodgkin & Huxley, 1952) and was awarded with the Nobel Prize in Physiology and Medicine in 1963. It involves four independent variables: one stands for the action potential producing spikes and bursts, and three for the probabilities of the membrane ion gates to be open or closed.

The set of dynamical equations corresponding to Hodgkin-Huxley (HH) model is given by (Hodgkin & Huxley, 1952):

$$\begin{aligned} C_M \cdot \frac{dv}{dt} &= -g_{Na} m^3 h \cdot (v - E_{Na}) - g_K n^4 \cdot (v - E_K) - g_{Cl} \cdot (v - E_{Cl}) + I \; ; \\ \frac{dm}{dt} &= \alpha_m \cdot (1 - m) - \beta_m \cdot m \; ; \\ \frac{dn}{dt} &= \alpha_n \cdot (1 - n) - \beta_n \cdot n \; ; \\ \frac{dh}{dt} &= \alpha_h \cdot (1 - h) - \beta_h \cdot h \; . \end{aligned} \tag{1}$$

Here $v(t)$ stands for the membrane potential, $m(t)$, $n(t)$, $h(t)$ are the membrane gate variables, and the control signal is represented by the sum $I(t)$ of external and synaptic currents entering the cell.

Here $\alpha_{m,n,h}$ and $\beta_{m,n,h}$ are fenomenologically found suitable rate positive coefficients related to the gate probabilities, they are given by:

$$\begin{aligned} \alpha_m(v) &= \frac{0.01 \cdot (25 - v)}{\exp\left\{\frac{25 - v}{10}\right\} - 1} \; ; \; \beta_m(v) = 4 \cdot \exp\left\{-\frac{v}{18}\right\} ; \\ \alpha_n(v) &= \frac{0.01 \cdot (10 - v)}{\exp\left\{\frac{10 - v}{10}\right\} - 1} \; ; \; \beta_n(v) = 0.125 \cdot \exp\left\{-\frac{v}{80}\right\} ; \\ \alpha_h(v) &= 0.07 \cdot \exp\left\{-\frac{v}{20}\right\} ; \; \beta_h(v) = \frac{1}{\exp\left\{\frac{30 - v}{10}\right\} + 1} \; . \end{aligned} \tag{2}$$

The set of constants in (1) includes the potentials E_{Na} (equilibrium potential at which the net flow of *Na* ions is zero), E_K (equilibrium potential at which the net flow of *K* ions is zero), E_{Cl} (equilibrium potential at which leakage is zero) in mV, the membrane capacitance C_M and the

conductivities g_{Na} (sodium channel conductivity), g_K (potassium channel conductivity), g_{Cl} (leakage channel conductivity) in mS/cm^2:

$$\begin{aligned} g_{Na} &= 120; \; E_{Na} = 115; \\ g_K &= 36; \quad E_K = -12; \\ g_{Cl} &= 0.3; \; E_{Cl} = 10.36. \end{aligned} \tag{3}$$

Dynamics of Hodgkin-Huxley neurons possesses variety of regular and chaotic regimes (Guckenheimer & Oliva, 2002; Horng & Huang, 2006; Wang, et al., 2011; Hoppensteadt, 2013). Being 4-dimentional, it covers the resting-and-spiking intermittency.

The model (1)-(3) has several features reflecting real properties of biological neurons:

a) It cannot spike itself without a stimulation by the external current I;

b) It has a threshold (Tonnelier, 2005), i.e. HH neuron can spike under the stimulation even with a constant current, but it must be greater than a certain minimum level.

The application of control algorithms to the single control parameter $I(t)$ allows to reproduce the variety of dynamical regimes in the model (1)-(3).

2. Control Algorithms for Hodgkin-Huxley Neuron Tracking

To track the dynamics of a single HH neuron we use here two alternative suboptimal algorithms: speed gradient and target attractor feedback. In both our approaches we force the HH system to follow (to track) the goal membrane potential functions and uses the stimulating current as an external control parameter.

2.1. Speed Gradient Algorithm

Speed gradient (SG) algorithm is based on the definition of the scalar target (goal) function (Fradkov & Pogromsky, 1998; Fradkov, 2007), that for the case of single neuron with one action potential can be defined as:

$$G = \frac{1}{2}\left[v(t) - v_*(t)\right]^2. \tag{4}$$

Here $v(t)$ is the actual membrane potential in the system (1), $v_*(t)$ is the target potential that must have a shape of smooth differentiable function. The goal of feedback control is achieved when

the target function G tends to zero. The target (4) following the goal membrane potential v_* as a given time-dependent function is called ***tracking***.

Let'stakethe time derivative of (4):

$$\Omega = \frac{dG}{dt} = (v - v_*)\left[\frac{dv}{dt} - \frac{dv_*}{dt}\right] . \quad (5)$$

The derivative dv/dt contains the control signal I through the RHS of the corresponding dynamical system (1).The algorithm defines the feedback control in a gradient form in the space of control signal. In the case of one neuron it is reduced to the partial derivative due to 1-dimensional character of the driving current I:

$$I_{SG} = -\gamma \frac{\partial \Omega}{\partial I} . \quad (6)$$

Here γ is a positive constant. By (1) it implies:

$$I_{SG} = -\frac{\gamma}{C_M}(v - v_*) . \quad (7)$$

Together with the system (1) the SG control algorithm (7) leads the evolution of the dynamical system to the attractor manifold described by the goal function (4).

2.2. Target Attractor Algorithm

Target attractor (TA) algorithm ("synergetic control" in author's terminology) is based on the "directed self-organization of the dynamical system" (Kolesnikov, 2012). The m-parametric attracting invariant manifold (the subset referring the control target)

$$\psi_s(x_1,...,x_n) = 0 ; \; s = 1..m \quad (8)$$

is defined as a functions of the state variables $x_1,\ldots,x_n$. Eqs(8) provide the asymptotic stability of the system dynamics with respect to the control target. To do it, let's require minimum of the following optimizing functional to be satisfied:

$$J = \int_0^\infty \left(\sum_{s=1}^{m} \left[T_s^2 \left(\frac{d\psi_s(t)}{dt} \right)^2 + \psi_s^2(t) \right] \right) dt = \min , \quad (9)$$

where T's are positive constants (time scales). To achieve the minimum (9) in exponent asymptotic we define the "synergetic" feedback as a set of s equations for the observers (Kolesnikov, 2014):

$$T\frac{d\psi_s(t)}{dt}+\psi_s(t)=0. \qquad (10)$$

Tending to zeros, the observers (8), (10) lead the dynamical evolution of the system to the target attractor.

Let's construct the target attractor feedback algorithm for the membrane action potential $v(t)$. For its tracking we define the goal function in the form:

$$\psi(t)=v(t)-v_*(t), \qquad (11)$$

with a given target potential $v_*(t)$. In the exponential form the "synergetic" feedback (10) is given by:

$$T\frac{d\psi}{dt}=-\psi, \qquad (12)$$

with a positive control constant T. That leads to:

$$\frac{dv}{dt}=\frac{dv_*}{dt}-\frac{1}{T}(v-v_*). \qquad (13)$$

The control signal I is restored from RHS of the dynamical system after the substitution (13) into (1):

$$I_{\mathrm{TA}}=C_M\cdot\left[\frac{dv_*}{dt}-\frac{1}{T}(v-v_*)\right]+g_{Na}m^3h\cdot(v-E_{Na})+g_Kn^4\cdot(v-E_K)+g_{Cl}\cdot(v-E_{Cl}). \qquad (14)$$

Eq.(14) together with thesystem (1) corresponds to the driven neuron tracked to the target action potential v_*.

2.3. Comparison of Speed Gradient and Target Attractor Algorithms

To emphasize the principle difference between two algorithms, SG and TA, one can express them in 'mechanical' terms. Speed gradient approach creates in the dynamical system an extra force that serves as a 'viscous friction'. It is off at the constant or dynamically changing target parameter level (action potential in our model). Far away from this level the 'friction' is large. Target attractor algorithm defines the attractor manifold, takes the dynamics of the system

into its neighborhood exponentially and forces the system to stay forever at the target attractor. Definitely, such a' hard' approach should be more efficient from the point of accuracy to compare with the 'soft' SG, but in the same time more energy consuming.

Both algorithms provide the robustness (Fradkov & Pogromsky, 1998; Kolesnikov, 2012): they do not depend sufficiently on the initial conditions and are stable under the relatively small external perturbations in the dynamics of the driven system (1). Both algorithms are sub-optimal: they are closed to the Pontryagin's optimal control locally.

3. Simulation of Tracking for Hodgkin-Huxley Neuron

Here we demonstrate numerically the efficiency of our both tracking algorithms via the example where the target membrane potential is formed by the set of harmonic functions with different amplitudes and different frequencies. The same tracking efficiency we observed in many numerical experiments for HH neuron tracking for different shapes of the target potential.

3.1. Tracking the Dynamics of HH Neuron via SG and TA Algorithms

The difference in the tracking for two algorithms is presented on Figure 1 for the target signal:

$$v_*(t) = \cos t - 3\cos(\sqrt{5}t - 2) + 3\cos(7t + 0.5) + \cos(\pi \cdot t + 1) - 0.3\cos\left(\frac{13}{21}t + 5\right) - 46\,. \quad (15)$$

The typical scales of the target function (15) reflect the features of real neurons. For both algorithms the control constants gamma and $1/T$ has been chosen as 0.05.

The goal of tracking is achieved in both algorithms: the actual (blue) and the red (target) voltages on Figure 1 are in good agreement.

At the points with the highest absolute value of the target potential derivative TA algorithm tracks the goal better.

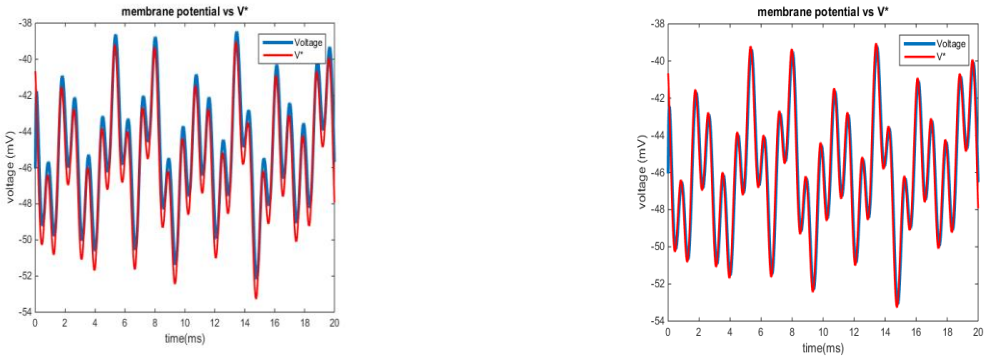

Figure 1: *Tracking for the linear superposition of harmonics (15). The target potential $v_*(t)$ is denoted by red color, the actual action potential $v(t)$ – by blue color.* ***Left:*** *speed gradient algorithm;* ***Right:*** *target attractor algorithm.*

On Figure 2 the tracking is performed for the combination of a burst-type function and the train of three Gaussian-shaped spikes:

$$v_*(t) = (\sin(8\pi t) + 6) \cdot \exp\left\{-\frac{(t-2)^2}{5}\right\} + \exp\left\{-\frac{(t-8)^2}{5}\right\} + \exp\left\{-\frac{(t-10)^2}{5}\right\} + \exp\left\{-\frac{(t-18)^2}{5}\right\} - 46 \,. \quad (16)$$

They correspond to a combination of bursting and spiking behavior in a real neuron.

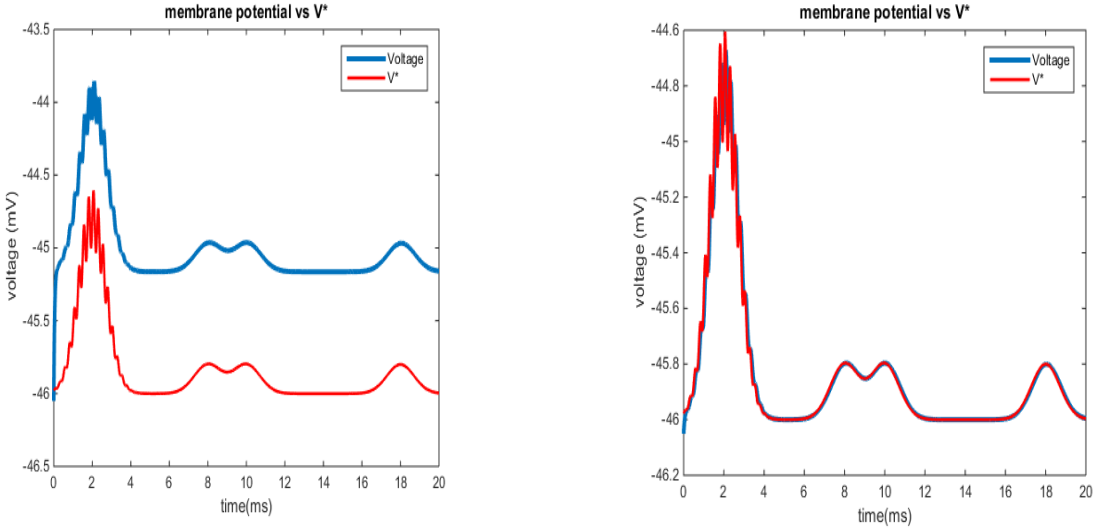

Figure 2: *Tracking for the burst-type pulse and the spike train (16). The target potential $v_*(t)$ is denoted by red color, the actual action potential $v(t)$ – by blue color.* ***Left:*** *speed gradient algorithm;* ***Right:*** *target attractor algorithm.*

One can easily see that the speed gradient algorithm can copy the arbitrary shape of the target potential, but it may have a systematic error between the actual action potential (the blue color

on Figs. 1-2) and its target (the red color on Figs. 1-2), see Section 3.2. Target attractor algorithm does not demonstrate such features.

The basic criteria for the comparison of SG and TA algorithms are the error of tracking and the energy efficiency.

3.2. Comparison of Tracking Error of SG and TA Algorithms for HH Neuron

The goal achievement of the tracking is evaluated by the error function:

$$e(t) = |v(t) - v_*(t)| \,. \tag{17}$$

It is plotted for the target function (15)-(16) on Figure 3.

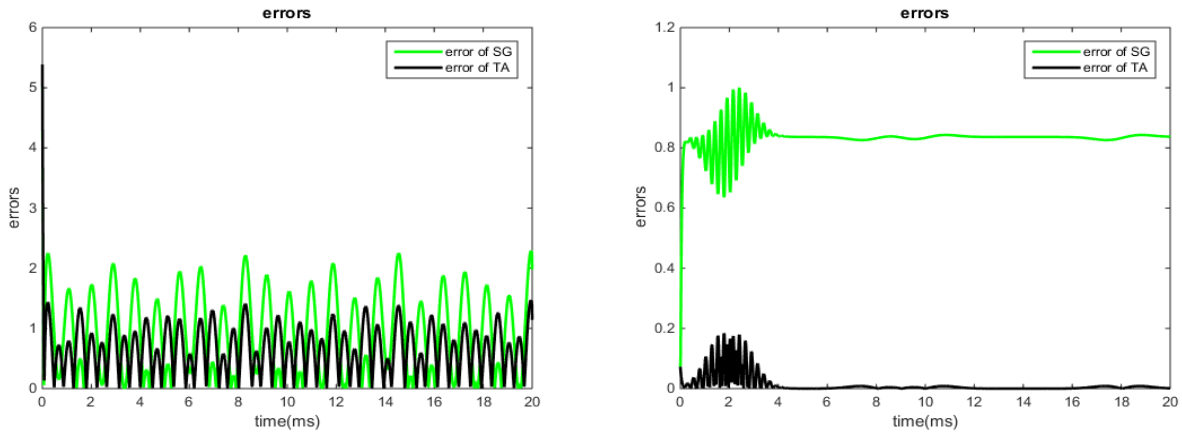

Figure 3: *Error of tracking e(t) for speed gradient (green) and target attractor (black) algorithms.* ***Left:*** *the linear superposition of harmonics (15);* ***Right:*** *the bursting-and-spiking train (16).*

On Figure 3 one can observe easily that the achievement of the goal may have a systematic error for the case of SG, especially for the spiking train case. It depends strongly on the control constant gamma in (6). This effect is observed forthe speed gradient algorithm only, see Figure 4 below. The target attractor algorithm leads to the tracking goal exponentially fast with the minor error.

We observe a systematic error for SG algorithm taking the target signal v_* as a constant, i.e. considering the case where the tracking goal is just a stabilization of the action potential at the certain level. The horizontal axis on Figure 4 represents different gammas (normalized by the capacitance C_M), while the vertical axis stands for the target stabilization level of the action potentials. The color marks the approximate number of oscillations for the dynamics of the

actual action potential $v(t)$ aroundthe stabilization level v_*. The deep blue asymptotic color corresponds to a perfect stabilization, while the deep red asymptotic color reflects non-decaying oscillations of the action potential around the target level that never leads to the stabilization.

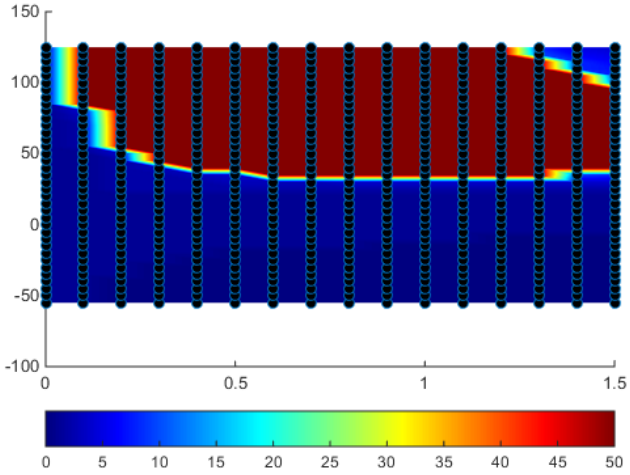

Figure 4: *The achievability of the control goal (4) in speed gradient algorithm for different control constants.* ***Horizontal axis:*** *gamma constant in (6);* ***Vertical axis:*** *the stabilization level v_*. The color marks the quality of the stabilization (see the explanations above).*

Thus, on Figure 4 one can easily see that the choice of the control parameter gamma must be in a good agreement with the target level of the action potential v_*, otherwise there is no the goal achievement (the red domain on the plot). The similar effect one can observe on the right plot of Figure 3 for SG case.

3.3. Energy Power Efficiency of SG and TA Algorithms

Another sufficient factor of successful control is the minimum power of the energy $P(t)$ that is pumped by the control field into the system per unit of time. For the HH electrical circuit model providing the dynamical system (1) it can be evaluated as:

$$P(t) = I(t)v(t). \tag{18}$$

For the particular cases (15) and (16) this power is plotted on Figure 5.

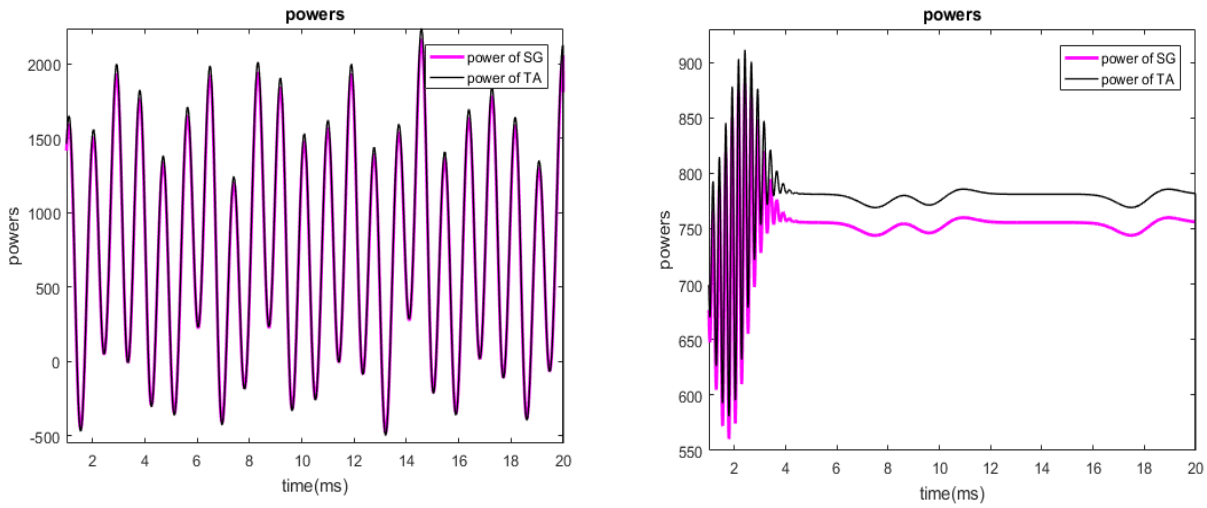

Figure 5: *Power of tracking P(t) for speed gradient (pink) and target attractor (black) algorithms.* ***Left:*** *the linear superposition of harmonics (15);* ***Right:*** *the bursting-and-spiking train (16).*

For the harmonic targets the powers of SG and TA signals do not differ sufficiently (the left plots). Nevertheless, for the spiking and bursting trains (the right plots) the target attractor algorithm is more energy consuming (its black curve of the energy pumping by control systematically stays above the SG pink curve).

3.4. Insensibility towards the Perturbation of the Initial Conditions

For real neurons we do not know exactly the set of the initial conditions for the dynamical variables (1). In the frame of SG and TA algorithms it is not sufficient, because the behavior of the dynamical system depends on the initial conditions very week (Fradkov, 2007; Kolesnikov, 2012). As an example, we demonstrate on Figure 6 the dynamics of the system (1) with few sets of its initial conditions under SG tracking (7); the target voltage is colored by red.

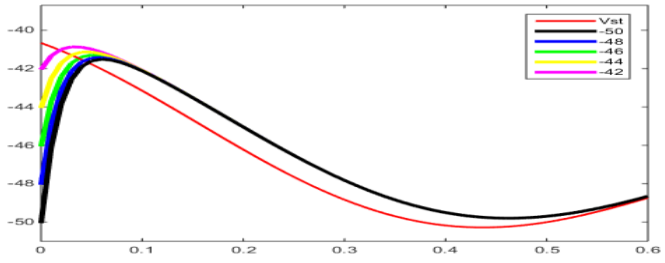

Figure 6: *SG tracking (7)of the target signal (red line) for different initial conditions;* ***Vertical axes:*** *the potentials in mV);* ***Horizontal axes:*** *time in ms.*

The Figure 6 shows that for all initial conditions the system dynamics converges to the target behavior.

4. Conclusions and Discussion

The comparison of two algorithms, speed gradient and target attractor, shows that the choice of the certain approach depends on the criteria of control:

- If the main factor is the minimization of the error (17), the target attractor method is definitely preferable.
- If we consider performing the control with the minimum possible energy than the speed gradient has the priority.

Two alternative algorithms developed here are not restricted by a single neuron. They could be used effectively for the purposes of neuro-informatics and for modeling neural dysfunctions like epileptiform or other abnormal behavior in Hodgkin-Huxley neuron clusters.

For the extension of our approach to multi-neuron networks with an arbitrary topologySG and TA algorithms for the control of spiking in the network models should consider also the detailed mechanisms of synaptic transmission (Lu, et al., 2017), spontaneous voltage oscillations(Neiman, et al., 2011) and different roles of neurons in controlling population (Bandopadhayay & Stiles, 2017). Their applications for the modeling of neural populations will provide:

- An efficient tool for studying the mechanisms of spiking and bursting in biological neuronal networks;
- A theoretical background for practical realization of real-time control in biological neuronal networks.

5. Acknowledgement

This work has been supported by TÜBİTAK (the Scientific and Technological Research Council of Turkey), Project no. 116F049 “Controlling Spiking and Bursting Dynamics in Hodgkin-Huxley Neurons”.

References

Ahmadian, Y., Packer, A. M., Yuste, R., Paninski, L. (2011). Designing optimal stimuli to control neuronal spike timing. *Journal of Neurophysiology*, 106(2), 1038-1053. https://doi.org/10.1152/jn.00427.2010

Awadalla M. H. A., Sadek, M. A. (2012). Spiking neural network-based control chart pattern recognition. *Alexandria Engineering Journal*, 51, 27-35. https://doi.org/10.1016/j.aej.2012.07.004

Bandopadhayay, P., Stiles, C. D. (2017). Population control: Cortical interneurons modulate oligodendrogenesis. *Neuron*, 94(3), 415-417. https://dx.doi.org/10.1016/j.neuron.2017.04.032

Bower, J. M. (Ed.). (2013). 20 Years of Computational Neuroscience. New York: Springer Sieser in Computational Neuroscience. https://doi.org/10.1007/978-1-4614-1424-7

Brody, C. D., Hopfield, J. J. (2003). Simple networks for spike-timing-based computation, with application to olfactory processing. *Neuron*, 37, 843-852. https://doi.org/10.1016/S0896-6273(03)00120-X

Cymbalyuka, G. S., Calabrese, R. L., Shilnikov, A. L. (2005). How a neuron model can demonstrate co-existence of tonic spiking and bursting. *Neurocomputing*, 6566, 869875. https://doi.org/10.1016/j.neucom.2004.10.107

Danzl, P., Moehlis, J. (2008). Spike timing control of oscillatory neuron models using impulsive and quasi-impulsive charge-balanced inputs. 2008 American Control Conference, Seattle, 171-176. https://doi.org/10.1109/ACC.2008.4586486

DiLorenzo, P. M., Victor, J. D. (Eds.). (2013). Spike Timing: Mechanisms and Function. Boca Raton: CRC Press. https://doi.org/10.1201/b14859

Ding, L., Hou, C. (2010).Stabilizing control of Hopf bifurcation in the Hodgkin-Huxley model via washout filter with linear control term. *Nonlinear Dynamics*, 60, 131-139. https://doi.org/10.1007/s11071-009-9585-x

Fourcaud-Trocme, N., Hansel, D., van Vreeswijk, C., Brunel, N. (2003). How spike generation mechanisms determine the neuronal response to fluctuating inputs. *The Journal of Neuroscience*, 23(37), 11628-11640.

Fradkov, A. L., Pogromsky, A. Yu. (1998). Introduction to Control of Oscillations and Chaos. Singapore: World Scientific. https://doi.org/10.1142/3412

Fradkov A. L. (2007). Cybernetical Physics: From Control of Chaos to Quantum Control. Berlin, Heidelberg: Springer.

Guckenheimer, J., Oliva, R. A. (2002). Chaos in the Hodgkin-Huxley model. *The SIAM Journal on Applied Dynamical Systems*, 1(1), 105-114. https://doi.org/10.1137/S1111111101394040

Haddad, W. M., Hui, Q., Bailey, J. M. (2014). Human brain networks: Spiking neuron models, multistability, synchronization, thermodynamics, maximum entropy production, and anesthetic cascade mechanisms. *Entropy*, 16, 3939-4003. https://doi.org/10.3390/e16073939

Hodgkin A. L., Huxley A. A. (1952). A quantitative description of membrane current and its application to conduction and excitation in nerve. *Journal of Physiology*, 117, 500-544.

Hoppensteadt, F. (2013). Heuristics for the Hodgkin-Huxley system. *Mathematical Biosciences*, 245(1), 56-60. https://doi.org/10.1016/j.mbs.2012.11.006

Horng, T.-L., Huang, M.-W.(2006). Spontaneous oscillations in Hodgkin-Huxley model. *Journal of Medical and Biological Engineering*, 26(4): 161-168. https://doi.org/10.1140/epjst/e2010-01282-3

Izhikevich, E. M. (2000). Neural excitability, spiking and bursting. *International Journal of Bifurcation and Chaos*, 10(6), 1171-1266. https://doi.org/10.1142/S0218127400000840

Jolivet, R., Lewis, T. J., Gerstner, W. (2003). The Spike Response Model: A Framework to Predict Neuronal Spike Trains. ICANN/ICONIP 2003, LNCS 2714, 846-853. https://doi.org/10.1007/3-540-44989-2_101

Kolesnikov, A. (2012). Synergetic Control Methods for Complex Systems. Moscow: URSS Publ.

Kolesnikov, A. (2014). Introduction of Synergetic Control.2014 American Control Conference, Portland, 3013-3016. https://doi.org/10.1109/ACC.2014.6859397

Lewis, J. E., Lindner, B., Laliberte, B., Groothuis, S. (2007). Control of neuronal firing by dynamic parallel fiber feedback: Implications for electrosensory reafference suppression. *Journal of Experimental Biology*, 210, 4437-4447. https://doi.org/10.1242/jeb.010322

Li, L., Brockmeier, A., Chen, B., Seth, S., Joseph T., Francis, J. T., Sanchez, J. C., Príncipe, J. C. (2013). Adaptive inverse control of neural spatiotemporal spike patterns with a

Reproducing Kernel Hilbert Space (RKHS) framework. *IEEE Transactions on Neural Systems and Rehabilitation Engineering*, 21(4), 532-543. https://doi.org/10.1109/TNSRE.2012.2200300

Lu, J., Tucciarone, J., Padilla-Coreano, N., He, M., Gordon, J. A., Huang, Z. J. (2017). Selective inhibitory control of pyramidal neuron ensembles and cortical subnetworks by chandelier cells. *Nature Neuroscience*, 20, 1377-1383. https://doi.org/10.1038/nn.4624

Lu, H., Balmer, T. S., Romero, G. E., Trussell, L. O. (2017). Slow AMPAR synaptic transmission is determined by stargazin and glutamate transporters. *Neuron*, 96(1), 73-80. http://dx.doi.org/10.1016/j.neuron.2017.08.043

Moss, F., Gielen, S. (2001). Neuro-Informatics and Neural Modelling, Amsterdam: Elsevier.

Nabi, A., Moehlis, J. (2012). Time optimal control of spiking neurons. *Journal of Mathematical Biology*, 64(6), 981-1004. http://dx.doi.org/10.1007/s00285-011-0441-5

Neiman, A. B., Dierkes, K., Lindner, B., Han, L., Shilnikov, A. L. (2011). Spontaneous voltage oscillations and response dynamics of a Hodgkin-Huxley type model of sensory hair cells. *The Journal of Mathematical Neuroscience*, 1, 1-24. https://doi.org/10.1186/2190-8567-1-11

Purali, N. (2002). Firing properties of the soma and axon of the abdominal stretch receptor neurons in the crayfish (*Astacusleptodactylus*). *General Physiology and Biophysics*, 21, 205-226.

Qiao, N., Mostafa, H., Corradi, F., Osswald, M., Stefanini, F., Sumislawska, D., Indiveri, G. (2015). A reconfigurable on-line learning spiking neuromorphic processor comprising 256 neurons and 128 K synapses. *Frontiers in Neuroscience*, 9, Article141. https://doi.org/10.3389/fnins.2015.00141

Qin, Y.-M., Wang, J., Men, C., Chan, W.-L., Wei, X.-L. Deng, B. (2013). Control of synchronization and spiking regularity by heterogenous aperiodic high-frequency signal in coupled excitable systems. *Communications in Nonlinear Science and Numerical Simulation*, 18(10), 2775-2782. https://doi.org/10.1016/j.cnsns.2013.02.010

Rabinovich, M. I., Abarbanel, H. D. I. (1998). The role of chaos in neural systems. *Neuroscience*, 87(1), 5-14. https://doi.org/10.1016/S0306-4522(98)00091-8

Rasmussen, R. G., Schwartz, A., Chase, S. M. (2017). Dynamic range adaptation in primary motor cortical populations. *Computational and Systems Biology, Neuroscience*, 6, e21409. https://doi.org/10.7554/eLife.21409.

Saha, A. K., Choudhury, S., Majumder, M. (2017). Performance efficiency analysis of water treatment plants by using MCDM and neural network model. *MATTER: International Journal of Science and Technology*, 3(1), 27 - 35. https://dx.doi.org/10.20319/Mijst.2017.31.2735

Schultheiss, N. W., Prinz, A. A., Butera, R. J. (2011). Phase Response Curves in Neuroscience: Theory, Experiment, and Analysis. New York: Springer Science & Business Media.

Strogatz, S. (1994). Nonlinear Dynamics and Chaos: With Applications to Physics, Biology, Chemistry, and Engineering. Massachusetts: Perseus Books Publishing.

Subashini, P., Dhivyaprabha, T. T., Krishnaveni, M. (2017). Cellular organism based Particle Swarm Optimization Algorithm for complex non-linear problems. *MATTER: International Journal of Science and Technology*, 3(2), 209 - 229. https://dx.doi.org/10.20319/mijst.2017.32.209229

Tonnelier, A. (2005). Categorization of neural excitability using threshold models. *Neural Computation*, 17(7), 1447-1455. https://dx.doi.org/10.1162/0899766053723087

Wang, J., Chen, L., Fei, X. (2007). Analysis and control of the bifurcation of Hodgkin-Huxley model. *Chaos, Solitons and Fractals*, 31(1), 247-256. https://doi.org/10.1016/j.chaos.2005.09.060